PREDICTION OF THE 2-D UNSTEADY SUPERCAVITY SHAPES

Vladimir N. Semenenko

National Academy of Sciences - Institute of Hydromechanics, Kyiv, Ukraine

Abstract

A method to calculate a length and a shape of two–dimensional unsteady supercavities past slender wedges and around slender hydrofoils is developed. In case of arbitrary time–dependence, the finite difference time discretization is used. For each time step, the solution is constructed by the method of integral equations. The variable supercavity length is found by numerical solving the equation of the mass of gas in the cavity balance. Examples of calculation of evolution of both the natural supercavity and the ventilated cavity in cases of aperiodic time–dependence and sinusoidal oscillation of hydrofoil are presented.

1 Introduction

Two–dimensional problems on supercavitation flow appear at investigation of supercavitating hydrofoils, struts, screws, turbomachinery blades *etc.* In the many cases the potential linearized theory is applied to calculate such flows (Tulin 1964).

At present, the problem of calculation of a two–dimensional unsteady cavity shape and length $l(t)$ has had no complete solution in case of the non–zero cavitation number $\sigma = 2(p_\infty - p_c)/\rho V_\infty^2$, where p_c is the cavity pressure. A difficulty consists in that a standard linearization procedure of the flow region and the boundary conditions does not result in the problem linearity on the whole when $\sigma \neq 0$, because variation of the unknown time-function $l(t)$ has order of unit when the flow perturbations are first–order small.

It is usual to consider that taking into account the cavity length variability weakly influences on the forces acting on the hydrofoil if the supercavity is sufficiently long. However sometimes calculation of changing the length, the shape and the volume of the unsteady supercavity is quite necessary. These are problems on stability and self–induced oscillation of the ventilated cavities (Silberman and Song 1961, Michel 1973), also problems on dynamics of inner flows containing supercavities (Acosta and Furuya 1979) *etc.*

This paper states a method of solving the pointed problem for arbitrary time dependence and for a practically important case of supercavitation flow around oscillating hydrofoils.

2 Unsteady Supercavitating Wedge

At first, we consider the problem on unsteady supercavitation flow past a slender wedge $y = \pm f(x,t)$ (Figure 1, a). The flow is assumed potential and symmetric about x-axis. The linearized flow region represents a plane with a slit along the interval $0 < x < l(t)$. On the sides of the slit, we have the following boundary conditions:

$$\varphi_y = \pm N f(x,t), \qquad 0 < x < 1;\ y = \pm 0, \tag{1}$$

$$\theta = N\varphi = \frac{\sigma(t)}{2}, \qquad 1 < x < l(t);\ y = \pm 0, \tag{2}$$

$$\varphi_y = \pm N F(x,t), \qquad 1 < x < l(t);\ y = \pm 0, \tag{3}$$

where $N = \partial/\partial t + \partial/\partial x$ is the linear differential operator; θ is the acceleration potential; $y = F(x,t)$ is the equation of the upper cavity boundary. Here and below, the dimensionless variables are used. The cavity

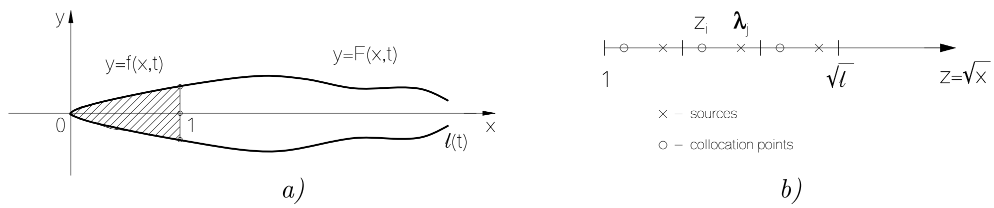

Figure 1: a) Unsteady supercavitating wedge. b) Scheme of discretization

length $l(t)$ is an unknown time function. The cavitation number σ is an unknown time function as well in the case of a gas–filled cavity.

Thus, in the general case we have the initial–boundary value problem that should be solved with the initial conditions: $\varphi(x,y,0)=\varphi_0(x,y)$, $l(0)=l_0$, $\sigma(0)=\sigma_0$.

3 Method of Integral Equations

The solution of that problem is constructed by the method of integral equations (Nishiyama 1972, Yefremov 1974). The symmetrical flow satisfying to the boundary condition (1)–(3) may be arranged when two–dimensional unsteady sources are distributed on the interval $[0, l(t)]$ of the x-axis. Their intensity $q(x,t)$ is equal to the normal fluid velocity φ_y jump at passage through the x-axis: $q(s,t)=2\varphi_y(s,t)$. Calculating the acceleration potential $\theta = N\varphi$ induced by all the sources and substituting it in the boundary condition (2) we obtain the singular integro–differential equation:

$$\int_0^{l(t)} \frac{q(s,t)\,ds}{x-s} + \frac{\partial}{\partial t}\int_0^{l(t)} q(s,t)\ln|x-s|\,ds - \pi\sigma(t) = 0, \qquad 1 < x < l(t). \tag{4}$$

Here, parts of the both integrals may be easily calculated from $s=0$ to $s=1$ because $q(x,t)=2Nf(x,t)$ when $0<x<1$.

It is easy to obtain the equation of the upper cavity boundary from the kinematic condition on the cavity boundary (3):

$$F(x,t) = N^{-1}\varphi_y(x,t) = \frac{1}{2}\int_0^{x} q(s,t-x+s)\,ds, \qquad 1 \le x \le l(t). \tag{5}$$

Since both the cavity length $l(t)$ and the cavity number $\sigma(t)$ are unknown time–functions in the general case, two relations are added to the equation (4):

1) the condition of solvability of the Newmann's external boundary value problem for the velocity potential $\varphi(x,y,t)$:

$$\int_0^{l(t)} q(s,t)\,ds = 0, \tag{6}$$

2) the equation of the mass of gas in the cavity balance for the ventilated cavities:

$$\frac{d}{dt}\big[\overline{p}_c(t)Q(t)\big] = \beta\big[\dot{q}_{in} - \dot{q}_{out}(t)\big], \tag{7}$$

where $\overline{p}_c(t)=p_c(t)/\sigma_0$; Q is the cavity area; $\beta=\sigma_v/\sigma \ge 1$ is the dynamic similarity parameter; σ_v is the natural vapor cavitation number; $\dot{q}_{in}$ is the volumetric air–supply rate into the cavity referred to p_∞; $\dot{q}_{out}(t)$ is the volumetric air–leakage rate from the cavity. We assume that the cavity pressure $p_c(t)$ changes synchronously along the cavity. From here, an estimation follows for admissible frequency of the unsteady process: $f << a_g/l_0$, where a_g is the sound speed in the vapor–gas medium filling the cavity.

Obtained set of three equations (4), (6) and (7) to determine three functions $q(x,t)$, $l(t)$ and $\sigma(t)$ must be integrated on time at the initial conditions $l(0) = l_0$, $\sigma(0) = \sigma_0$, $q(x,0) = q_0(x)$. We note that application of the condition (6) ensures boundedness of the pressure at infinity. In the particular case of steady flow, the equation (6) is a condition of the cavity closure. In the case of unsteady flow, the cavity is unclosed.

4 Numerical Algorithm

The set of the equations (4), (6) and (7) is non–linear because the cavity length $l(t)$ is the unknown time–function. Its solution is sought numerically in sequential moments $t^{(n)} = t^{(n-1)} + \Delta t, \quad n = 2, 3, \ldots$ with the starting conditions $t^{(1)} = 0$, $q^{(1)}(x) = q_0(x)$, $l^{(1)} = l_0$, $\sigma^{(1)} = \sigma_0$. The time derivative in the equation (4) is approximated by finite difference of the first order. Then, for the n-th time step the equations (4) and (6) may be written in the form:

$$\int\limits_1^{l^{(n)}} \frac{q^{(n)}(s)\,ds}{x-s} + \frac{1}{\triangle t}\int\limits_1^{l^{(n)}} q^{(n)}(s)\ln|x-s|\,ds - \pi\sigma^{(n)} = A_1^{(n)}(x) + \frac{1}{\triangle t}A_2^{(n-1)}(x), \qquad 1 < x < l^{(n)}. \tag{8}$$

$$\int\limits_1^{l^{(n)}} q^{(n)}(s)\,ds = A_3^{(n)} = -2\int\limits_0^1 Nf^{(n)}(s)\,ds, \quad \text{where} \quad A_2^{(n-1)}(x) = \int\limits_1^{l^{(n-1)}} q^{(n-1)}(s)\ln|x-s|\,ds. \tag{9}$$

Here, the function $A_1^{(n)}(x)$ is known if the the wedge unsteady shape $f(x,t)$ is given. For each iteration, the value $l^{(n)}$ is considered to be known, then the set of equations (4), (6) with respect to $q^{(n)}(s)$, $\sigma^{(n)}$ is linear. It is solved numerically by the method of discrete singularities (Yefremov 1974).

The numerical method of discrete singularities consists in approximation of the integral equations (8), (9) by set of the linear algebraic equations by replacing the continuous distribution of the sources along the x-axis by the discrete one and applying the quadrature formulae. To improve the method convergence, the change of variables is realized in the integrals: $x \to z^2$, $s \to \lambda^2$. The discrete source and the collocate points, where the boundary condition is satisfied, are located in each partition interval. The sourse location λ_j and the collocation point location z_i are defined by a function class in which the solution of the singular integral equation (8) is sought (Figure 1, b):

$$z_i = 1 + \triangle z(i - 0.75), \qquad \lambda_j = 1 + \triangle z(j - 0.25), \qquad \triangle z = \frac{\sqrt{l^{(n)}} - 1}{M}, \qquad i,j = 1,2,\ldots,M. \tag{10}$$

As a result, we obtain the set of $M+1$ linear algebraic equations:

$$\triangle z \sum_{j=1}^{M} q_j^{(n)} \left(\frac{\triangle t}{z_i^2 - \lambda_j^2} + \ln|z_i^2 - t_j^2| \right) t_j - \frac{\pi \triangle t}{2}\sigma^{(n)} = \frac{\triangle t}{2} A_1^{(n)}(z_i) + A_2^{(n-1)}(z_i), \tag{11}$$

$$\triangle z \sum_{j=1}^{M} q_j^{(n)} \lambda_j = \frac{1}{2} A_3^{(n)}, \qquad i = 1,2,\ldots,M.$$

5 Unsteady Natural Vapor Supercavity

In the case of a natural vapor supercavity the equation (7) transforms into condition of the cavity pressure to be constant: $\sigma = \sigma_0 = \text{const}$.

Figure 2 gives examples of calculation of history of the natural vapor supercavity length with changing the wedge angle (pitching oscillation of wedge) when $l_0 = 5.0$. The corresponding quasistationary dependencies of $l(t)$ are plotted by dashed lines for comparison. They are calculated by omitting the time derivatives in both the equation (4) and the relation (1).

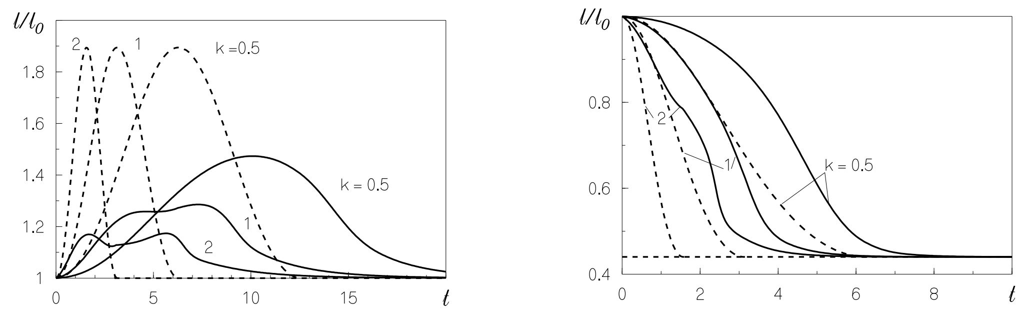

a) *b)*

Figure 2: History of the supercavity length at variation of the wedge angle. a) Impulse increasing of angle. b) Regular decreasing of angle

In graphs of Figure 2, a, the wedge angle increases in 1.5 times for different time intervals t_p (*i.e.* at different frequency of the process $k = \pi/t_p$) and then decreases to its initial value. A comparison with quasistationary behavior of $l(t)$ allows to note the following peculiarities of the unsteady supercavity behavior:

1) increase and decrease of the cavity length occur asymmetrically;

2) the cavity length is changed the less the less is duration of perturbation (*i.e.* the more is the impulse frequency k);

3) the function $l(t)$ change becomes non–monotone at sufficiently high values of the impulse frequency k.

In graphs of Figure 2, b, the wedge angle decreases in 2 times for different the process frequency k. As a result, the cavity length decreases from $l_0 = 5.0$ to the new balanced magnitude $l_1 = 2.2$. One can see that the cavity attains the balanced length with the more time lagging the more value of k.

One can see that it is necessary to store only M values of the function $A_2^{(n-1)}$ for previous time step for calculation of the function $l(t)$ in case of a natural vapor supercavity. However, values of the function $q_j^{(m)},\ \ j = 1, 2, \ldots, M$ for the $m \sim l^{(n)}/\triangle t$ previous time steps are used for calculation of a unsteady cavity shape $F(x,t)$ by the equation (5) due to lagging character of the integrand. Also, that is right in case of calculation of a unsteady ventilated supercavities by using the equation (7).

However, one can see that the following relation is fulfilled for the unsteady cavity shape:

$$F_i^{(n)} = F_{i-1}^{(n-1)} + \frac{\triangle x}{2}\, q_i^{(n)}, \qquad i = 1, 2, \ldots, M. \tag{12}$$

Thus, it is enough to store one–dimensional array $F_i^{(n-1)}$ to calculate the cavity shape $F_i^{(n)}$ for the n-th time step. Moreover, it is obvious that the total characteristic always has the more smoothness that the distributed one. In this case the calculation accuracy increases, and the calculation algorithm becomes pretty economical.

6 Sinusoidal Perturbations

The described numerical algorithm may be considerably simplified for the practically important case of periodic time dependence of the flow. In this case, simplification is reached due to bringing the time derivative within the integral of the equation (4) and using the exponential representation of the time dependence for all the functions having the variation order $O(\varepsilon)$:

$$f(x,t) = \alpha_0\, x + \kappa\, \mathrm{Re}\{f^*(x)\, e^{jkt}\}, \qquad q(x,t) = \alpha_0\, q_0(x,l) + \kappa\, \mathrm{Re}\{q^*(x,l)\, e^{jkt}\},$$

$$\sigma(t) = \alpha_0\, \sigma_0(l) + \kappa\, \mathrm{Re}\{\sigma^*(l)\, e^{jkt}\}, \qquad F(x,t) = F_0(x,l) + \kappa\, \mathrm{Re}\left\{F^*(x,l)\, e^{jkt}\right\},$$

where $\alpha_0 \sim \kappa \sim O(\varepsilon)$; $||f^*|| \sim ||q_0|| \sim ||q^*|| \sim ||\sigma_0|| \sim ||\sigma^*|| \sim ||F_0|| \sim ||F^*|| \sim O(1)$; k is the reduced frequency. The values which are marked by a star are complex with respect to j (the complex amplitudes). The functions $q_0(x,l)$, $q^*(x,l)$ *etc.* depend on the unsteady cavity length $l(t)$ like on a parameter. In this

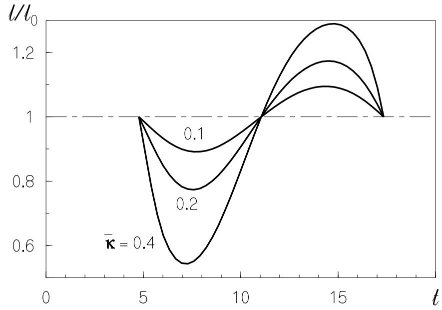

Figure 3: Effect of amplitude of the wedge oscillation on $l(t)$ $(l_0 = 6.0, \; k = 0.5;$ wave–shaped deformation)

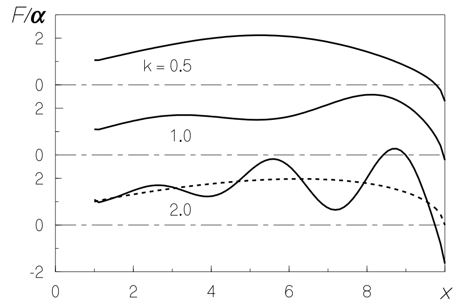

Figure 4: Supercavity shape at several oscillation frequencies: $(l_0 = 10.0, \; \overline{\kappa} = 0.1;$ pitching oscillation of wedge)

case some error is introduced into the solution that rapidly decreases with increasing the average cavity length.

We obtain the set of the singular integral equations from the equations (4), (6) to determine unknown perturbations $q^*(x)$ and σ^* for each time step:

$$\int_1^{l^{(n)}} q^*(s)\left(\frac{1}{x-s} + jk\ln|x-s|\right) ds - \pi\sigma^* = -2\int_0^1 \varphi_y^*(s)\left(\frac{1}{x-s} + jk\ln|x-s|\right) ds, \tag{13}$$

$$\int_1^{l^{(n)}} q^*(s)\, ds = -2\int_0^1 \varphi_y^*(s)\, ds, \quad \text{where} \quad \varphi_y^*(s) = \left(jk + \frac{d}{ds}\right) f^*(s). \tag{14}$$

The integrals in right parts of the equations (13) and (14) are easy calculated for concrete form of oscillations of the wedge sides. After separating a real part and a imaginary part of the equations (13), (14) and discretization, we obtain a set of $2(M+1)$ linear algebraic equations for each time step.

In the case of periodic perturbations we have for the cavity shape when $t = t^{(n)}$, $l = l^{(n)}$:

$$\frac{F_0(x,l)}{\alpha} = \frac{2}{\pi}\left[\frac{\sqrt{l(x-1)(l-x)}}{l-1} + x\arctan\sqrt{\frac{l-x}{l(x-1)}}\right], \qquad F^*(x,l) = \frac{1}{2}\, e^{-jkx}\int_0^x q^*(s,l)\, e^{jks}\, ds. \tag{15}$$

Figure 3 gives graphs of dependencies $l(t)$ calculated for only oscillation period at different values of the relative amplitude of forced oscillations $\overline{\kappa} = \kappa/\alpha_0$. When the reduced frequency k and perturbation amplitude $\bar{\kappa}$ increase, the cavity length oscillation differs more and more from the sinusoidal one. The functions $l(t)$ and $Q(t)$ become discontinuous when exceed some critical values of k and $\bar{\kappa}$.

Figure 4 shows characteristic wave–shape of the cavity past the oscillating wedge for three values of the frequency k. For convenience of comparison, in each case the cavity shape was calculated by the formula (15) in instant t_k when $l(t_k) = l_0$. The closed steady cavity shape, when $k = 0$, is shown by dashed line. When $k > 0$, the cavity is unclosed.

One can see that character of the cavity boundary deformations is the same for different types of oscillations of the wedge sides. The kinematic waves created by oscillations of points of the cavity boundary separation propagate along the cavity with the velocity V_∞. Their amplitude increases approximately by a linear law.

7 Effect of Gas Filling the Ventilated Cavity

Numerous experiments demonstrate considerable difference between unsteady behaviour of natural supercavities and ventilated ones (*e.g.* Brennen *et al* 1980). The equation (7) shows that peculiarities of unsteady gas–filled ventilated cavities are conditioned by effect of two factors:

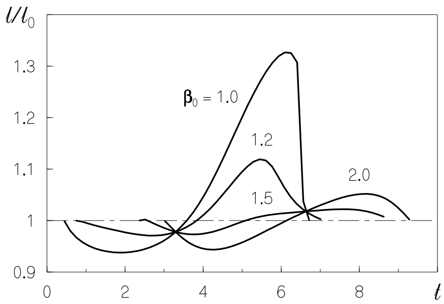

Figure 5: Influence of the parameter β_0 on $l(t)$ ($l_0 = 6.0$, $k = 1.0$, $\overline{\kappa} = 0.2$; wave–shaped deformation of wedge)

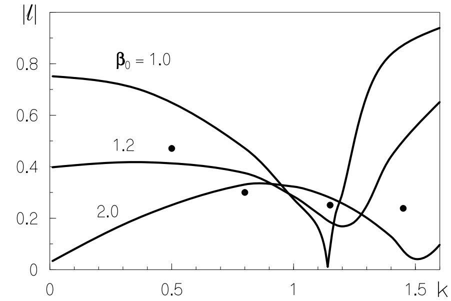

Figure 6: Influence of the parameter β_0 on frequency response of $l(t)$ ($l_0 = 4.8$, $\overline{\kappa} = 0.11$; pitching oscillation of wedge)

1) elasticity of gas filling the cavity. Its significance increases with increasing the similarity parameter $\beta > 1$;

2) law of gas–leakage from the cavity, *i.e.* dependence $\dot{q}_{out}(p_c)$. As experience was shown (Logvinovich 1973), it considerably depends on the Froude, Reynolds and Weber numbers. The gas–leakage process can not be exactly described by the potential theory. Therefore, we have to use semi–empirical and empirical relations in calculations.

Experimental data of Silberman and Song (1961) testify that for plane ventilated supercavities the air–supply rate may be approximated by the linear function (in the dimensional form):

$$\dot{q}_{out} = \gamma b_0 V_\infty \left(1 - \frac{\sigma}{\sigma_v}\right), \tag{16}$$

where $\gamma = 2.5 \cdot 10^{-4}$ is the empirical coefficient; b_0 is the width of the middle cavity section. In the case of a unsteady cavity we assume that the air–leakage rate depends on $\sigma(t)$ in quasi–stationary way.

Figure 5 shows graphs of the function $l(t)$ for different values of the parameter β_0. Influence of the parameter β_0 consists in increasing the phase lagging and changing the oscillation amplitude.

Figure 6 shows influence of the parameter β_0 on frequency response of the cavity length $|l|(k)$. The calculation parameters were chosen maximally corresponding to conditions of the experiments by Nishiyama (1982).

Since character of the cavity unsteady deformation is the same for different types of the foil oscillation, the experimental data by Nishiyama (1982) for hydrofoils may be compared with calculation of supercavity past the symmetric wedge. In Figure 6, the experimental data for semi–range of the cavity length oscillations, which are taken from the work by Nishiyama (1982), are plotted by circles.

The performed calculations allow to conclude that the influence of elasticity of the gas filling the cavity increases with increasing the parameter β_0. It was shown in the works Semenenko (1996a, 1998) that the 2-D gas–filled supercavity is unstable when $\beta > 3.08$. The proposed calculation method for forced oscillations is applicable at least for stable cavities, *i.e.* when $\beta < 3$ and $k < 2\pi/(l_0 - 1)$.

8 Unsteady Supercavitating Hydrofoil

In the case of non–symmetric flow around the supercavitating hydrofoil, the vortices of intensity $\gamma(x,t)$ are distributed on the interval $[0,1]$ together with the sources on the interval $[0, l(t)]$ of the x-axis (Figure 7).

In the case of sinusoidal oscillation of the hydrofoil, the set of two singular integral equations with respect to unknown intensities $\gamma^*(x)$ and $q^*(x)$ has been obtained before when $l = \text{const}$ (Yefremov 1974):

$$q^*(x) + \frac{1}{\pi}\int_0^1 \gamma^*(s)\left[\frac{1}{x-s} - k e^{jk(s-x)}\Big(\mathrm{si}\big(k(s-x)\big) + j\,\mathrm{ci}\big(k(s-x)\big)\Big)\right] ds = -\varphi_y^*(x), \quad 0 < x < 1, \tag{17}$$

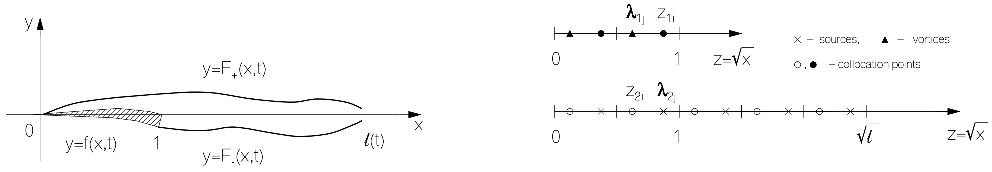

a) *b)*

Figure 7: a) Unsteady supercavitating hydrofoil. b) Discretization scheme

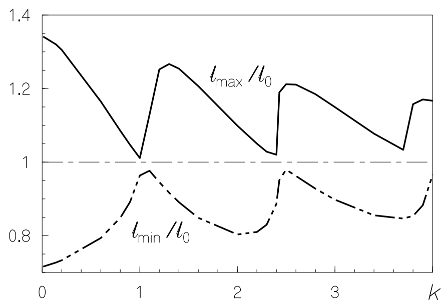

Figure 8: Oscillation range of $l(t)$ versus the oscillation frequency ($l_0 = 5.0$, $\overline{\kappa} = 0.2$; wave–shaped deformation of hydrofoil)

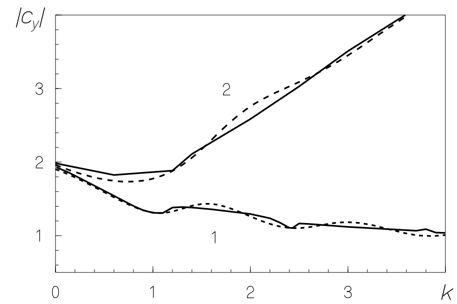

Figure 9: Frequency response of $c_y(t)$ for the unsteady supercavitating hydrofoil. 1 – Wave–shaped deformation; 2 – heaving oscillation

$$H(1-x)\gamma^*(x) + \frac{1}{\pi}\int\limits_0^{l^{(n)}} q^*(s)\left(\frac{1}{x-s} + jk\ln|x-s|\right) ds - \sigma^* = 0, \qquad 0 < x < l^{(n)}, \tag{18}$$

where $H(x) = 0$ when $x < 0$, $H(x) = 1$ when $x \geq 0$; $\mathrm{si}(x)$ and $\mathrm{ci}(x)$ are the integral sine and cosine (Abramovitz and Stegun 1964). Also, the equations (6) and (7) should be added to the equations (17) and (18) to determine the cavitation number σ^* and the cavity length $l(t)$.

Projections of the hydrofoil and the cavity are divided on N and $N + M$ intervals respectively. The discrete vortex location λ_{1j} and the collocation point location z_{1i} on the hydrofoil are (Figure 7, b):

$$z_{1i} = 1 + \frac{1}{N}(i - 0.25), \qquad \lambda_{1j} = 1 + \frac{1}{N}(j - 0.75), \qquad i, j = 1, 2, \ldots, N. \tag{19}$$

A location of the discrete sources λ_{2j} and the collocation points z_{2i} on the cavity, where the dynamical boundary condition is satisfied, is the same as in (10). As a result, after separating a real part and a imaginary part of the equations (13), (14), we obtain a set of $2\,(2N + M + 1)$ linear algebraic equations for each time step. The coefficient of the lift acting on the hydrofoil is:

$$c_y(t^{(n)}) = 2\alpha\int\limits_0^1 \gamma_0(s, l^{(n)})\,ds + 2\kappa\,\mathrm{Re}\Big\{e^{jkt}\int\limits_0^1 \gamma^*(s, l^{(n)})\,ds\Big\}. \tag{20}$$

In Figure 8, the range of oscillation of the function $l(t)$ in dependence on the reduced frequency k are given. Calculations showed that the range of oscillations of $l(t)$ has maximums close to the fundamental frequencies of a gas–filled supercavity (Semenenko 1996a).

In Figure 9, a comparison of frequency responses of $c_y(t)$ calculated when $l = \mathrm{const}$ (dashed lines) and with taking account of $l(t)$ (solid lines) is given. One can see that taking into account the cavity length variability results in smoothing the frequency response of c_y.

In Semenenko (1999), calculation of the oscillating supercavitating hydrofoil under a free water surface is presented.

9 Conclusions

The proposed method to calculate a length and a shape of 2-D unsteady supercavities gives results corresponding with experimental data at the non very high oscillation frequency k and the moderate relative amplitudes $\overline{\kappa}$. It may be applied at least for the values of dynamic parameter β corresponding to the stable cavities and for the oscillation frequencies which are lower than the lowest fundamental frequency of the cavity (Semenenko 1996a).

Presence of gas in the ventilated supercavity results in considerable changing the frequency responses of each of the functions $l(t)$, $Q(t)$ and $\sigma(t)$. Significance of elasticity of the gas filling the cavity increases with increasing the similarity parameter β.

Taking into account of the cavity length variability results in smoothing the frequency responses of the forces acting on the hydrofoil. The amplitudes of the force oscillations change weakly in comparison with the calculation when $l = \text{const}$. Thus, use of simple linear algorithms with $l = \text{const}$ is admissible to calculate the unsteady forces on hydrofoils as *e.g.* in Semenenko (1981).

A comparison of unsteady behavior of the mathematical models of 2-D and axisymmetrical supercavities shows their qualitative similarity. This confirms adequacy of the G.V.Logvinovich's principle of independence of the cavity section expansion (Logvinovich 1973), which is a basis of the mathematical model of the unsteady axisymmetric supercavities (*e.g.* Semenenko 1996b, Savchenko *et al* 2000).

References

Abramovitz, M., and Stegun, I. (Editors) 1964 *Handbook of Mathematical Functions with Formulae, Graphs and Mathematical Tables.* National Bureau of Standards, Applied Mathematics Series.

Acosta, A.J., and Furuya, O. 1979 A brief note on linearized, unsteady, supercavity flows. *Journal of Ship Research.* **23** (2), 85–88.

Brennen, C., Oey, K.T., and Babcock, C.D. 1980 Leading–edge flutter of supercavitating hydrofoils. *Journal of Ship Research.* **24** (3), 135–146.

Logvinovich, G.V. 1973 *Hydrodynamics of Flows with Free Boundaries.* Halsted Press.

Michel, J.M. 1973 Ventilated cavities: A contribution to the study of pulsation mechanism. Unsteady water flows with high velocities. Proc. of International Symp. IUTAM, Moscow: Nauka Publishing House, 343–360.

Nishiyama, T. 1972 Unsteady supercavitating hydrofoil theory at non-zero cavitation number. *Technology Reports, Tohoku Univ.* **37** (2), 259–282.

Nishiyama, T. 1982 Unsteady cavity flow model for two–dimensional super-cavitating hydrofoils in oscillation. *Technology Reports, Tohoku Univ.* **46** (2), 199–216.

Savchenko, Yu.N., Semenenko, V.N., and Putilin, S.I. 2000 Unsteady supercavitated motion of bodies. *Int. J. of Fluid Mechanics Research.* **27** (1), 109–137.

Semenenko, V.N. 1981 Unsteady flow around slender hydrofoil in artificial cavitation regime. *Journal of Hydromechanics.* (43), 20–29 (in Russian).

Semenenko, V.N. 1996a Instability of a plane ventilated supercavity in an infinite stream. *International Journal of Fluid Mechanics Research.* **23**, (1 & 2), 134–143.

Semenenko, V.N. 1996b Computer modeling of pulsations of ventilated supercavities. *International Journal of Fluid Mechanics Research.* **23**, (3 & 4), 302–312.

Semenenko, V.N. 1998 Instability and oscillation of gas–filled supercavities *Proc. Third International Symp. on Cavitation*, Grenoble, France. **2**, 25–30.

Semenenko, V.N. 1999 Unsteady flow calculations past ventilated hydrofoils. *Proc. Seventh International Conf. on Numerical Ship Hydrodynamics*, Nantes, France.

Silberman, E., and Song, C.S. 1961 Instability of ventilated cavities. *J. of Ship Research.* **5** (1), 13–33.

Tulin, M.P. 1964 Supercavitating flows – small perturbation theory. *J. of Ship Research.* **7** (3), 16–37.

Yefremov, I.I. 1974 *Linearized Theory of Cavitation Flow.* Kiev: Naukova Dumka Publishing House (in Ukrainian).